Ab initio and DFT modelling of complex materials: towards the understanding of electronic and magnetic properties of polyoxometalates

Josep M. Poblet,* Xavier López and Carles Bo

Departament de Química Física i Inorgànica, Universitat Rovira i Virgili, Imperial Tàrraco 1, 43005 Tarragona, Spain. E-mail: poblet@quimica.urv.es

Received 19th February 2003
First published as an Advance Article on the web 12th June 2003

In this review we summarise the quantum chemistry studies carried out by several groups over the last ten years on polyoxometalates, or polyoxoanions. This is an immense family of compounds made up of transition metal ions in their highest oxidation state and oxo ligands. The continuous progress of computers in general, and quantum chemistry software in particular, has enabled a number of topics in polyoxometalate chemistry to be studied from the electronic structure of the most representative polyoxometalate, the so-called Keggin anion, to the factors governing the inclusion complexes and the magnetism in reduced complexes.

1 Introduction

The first polyoxometalate (POM), the phosphomolybdate $[PMo_{12}O_{40}]^{3-}$, was reported by Berzelius in 1826 and, about 100 years later, Keggin solved the structure of the related anion $[PW_{12}O_{40}]^{3-}$.[1] Since then countless structures have been synthesised and characterised. Today, POMs constitute an immense class of polynuclear metal–oxygen clusters[2,3] usually formed by Mo, W or V and mixtures of these elements. POMs have potential applications in many fields including medicine, catalysis, multifunctional materials, chemical analysis, *etc*. According to Katsoulis' compilation,[4] in 1996 there were more than 700 communications (publications and patents) in the field of POMs. Most of their applications are related to the special ability of many POMs to accept one or several electrons with minimal structural changes.

Computational Transition Metal Chemistry has reached its maturity, basically thanks to the widespread acceptance of methods based on the density functional theory (DFT). In the seventies, the *ab initio* Hartree–Fock (HF) approximation provided a reasonable starting point for understanding reaction mechanisms involving small organic molecules. Later, Møller–Plesset perturbation theory, configuration interaction, coupled cluster theory and other methods provided a more quantitative description. For transition metals, the error in HF methods, the

Josep M. Poblet was born in Valls (Spain) in 1956. He was awarded his undergraduate degree in Chemistry in 1979 from the University of Barcelona and obtained his PhD in 1983 from the same university under the supervision of Professor Enric Canadell. In 1984, he did a postdoctoral stay with Professor Marc Bénard at the Louis Pasteur University in Strasbourg and in 1986 he became Assistant Professor in Physical Chemistry at the Rovira i Virgili University (Tarragona). He is currently Professor of Physical Chemistry and Head of the Department of Inorganic and Physical Chemistry at this university. His research field is theoretical inorganic chemistry with special interest in polyoxoanions, metallocarbohedrenes, metalofullerenes and complexes with high nuclearity.

Josep M. Poblet

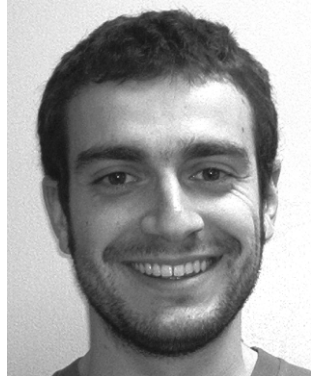

Xavier López

Xavier López was born in Barcelona in 1975. He studied Chemistry at the University of Barcelona, where he was awarded his undergraduate degree in 1999. In the same year he joined the research group of Professor Josep M. Poblet at the Rovira i Virgili University in Tarragona, where he began his PhD with a study of the general properties of polyoxometalates using density functional methods.

Carles Bo was born in El Vendrell (Spain) in 1963. He was awarded his BSc degree in Chemistry in 1986 from the University of Barcelona and his MSc degree in 1988 for experimental work in homogeneous catalysis under the direction of Professor Carmen Claver. In 1992 he was awarded a PhD by the same university under the supervision of Professor Josep M. Poblet. Since then he has been a member of Professor Poblet's group. He obtained an Assistant Professor position in Physical Chemistry at the Rovira i Virgili University in 1995. His research interest lies in the study of transition metal systems by computational methods, with special attention in the modelling of the homogeneous catalysis.

Carles Bo

DOI: 10.1039/b109928k

so-called *correlation energy*, is generally too large. Part of the correlation energy can be introduced using DFT methods. These give reliable structures and bonding energies with only moderate computational effort. Many organometallic and polynuclear structures have been described using DFT.[5] However, the number of high-level computational studies on POMs is still quite low. A combination of three factors—the large size of polyoxoanions, the presence of transition metal ions and the high negative charge—produce, in practice, important computational limitations. In the last ten years, a few groups have been especially active and have made important progress in describing and rationalising the electronic and magnetic properties of POMs. The first studies by Bénard were at the HF level. Later investigations preferentially used density functional methods, as implemented in the ADF set of programs.[6] In this paper, we review the most significant theoretical studies in the field of POMs. To do this, we concentrate more on the results achieved and less on the methods used.

2 Electronic structure and bonding in fully oxidised polyoxometalates

The most representative POM is the Keggin heteropolyanion (HPA), the formula of which is $[XM_{12}O_{40}]^{n-}$, where M is usually W^{6+} or Mo^{6+} and X, the *heteroatom*, is a main group or transition metal ion (P^{V}, Si^{IV}, Al^{III}, Ge^{IV}, Fe^{III}, Co^{II}, Co^{III}, Cu^{I}, Cu^{II}, *etc.*). The Keggin anion is made of an assembly of twelve MO_6 octahedrons sharing their corners or edges with a central XO_4 tetrahedron (Figure 1). The metal–oxygen bonds in such a

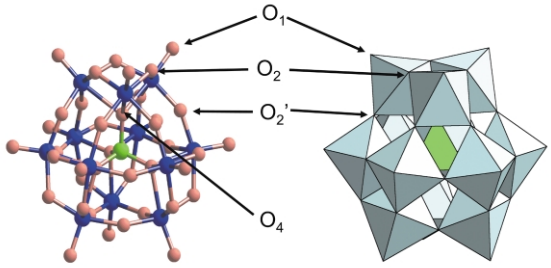

Fig. 1 Ball and stick and polyhedral representation for an α-$[XM_{12}O_{40}]^{n-}$ Keggin anion. Blue and green identify cations while red is used for oxo ions.

framework can be divided into three sets according to whether their oxygen atoms are tetrahedral (tetra), bridging (brid) or terminal (term). There is a fourth M–O bond type between the heteroatom and O(tetra). We will also use the notation O_m, where *m* indicates the number of ions bonded to the oxygen, throughout the text where it is convenient to do so. In the α-isomer, all metal centres are equivalent and the symmetry of the molecule is T_d. Marignac discovered a second isomer, today known as beta and with idealised C_{3v} symmetry. This differs from the α form in that there is a 60° rotation of one of the four edge-sharing M_3O_{13} triads. The common partial reduction of the *addenda* or *peripheral* M centres yields the intensely coloured "heteropoly blues". This term is normally used for reduced polyanions irrespective of their true colour.

Throughout this review we will use an abbreviated notation without oxygen atoms, charge or brackets, *e.g.*, PW_{12} for $[PW_{12}O_{40}]^{3-}$ and $PW_{12}1e$ for $[PW_{12}O_{40}]^{4-}$, where *n*e identifies the number of electrons in the metal orbitals, or *blue* electrons. For clusters with paramagnetic ions, the explicit oxidation state of the heteroatom is given: $Co^{II}W_{12}1e$ represents a heteropolyblue with one delocalised electron among the twelve tungstens and the central cobalt ion in the oxidation state of +2.

In general, DFT calculations reproduce the geometry of HPAs very well. The exception are the M=O(term) bond lengths, which are systematically longer than the experimental ones. The theoretical deviations in the M=O(term) bond lengths in Keggin and Wells–Dawson structures have been found, on average, 0.05 Å using the BP86 functional. This discrepancy between the X-ray and the computed geometries is somewhat smaller in isopolyanions such as $[M_6O_{19}]^{2-}$ (M = Mo and W),[7] and $[W_{10}O_{32}]^{4-8}$ using local functionals. Schematic representations for several typical POMs are given in Figure 2. For the

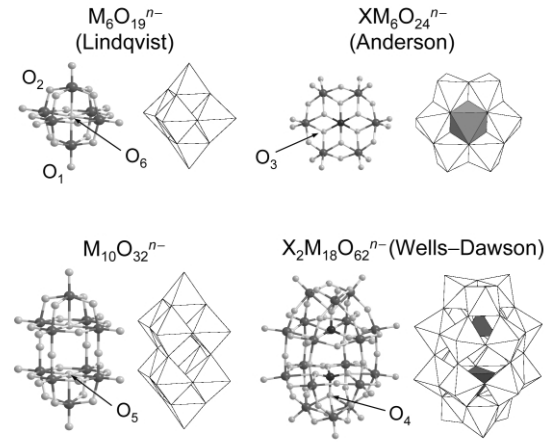

Fig. 2 Representation and oxygen labelling for several typical polyanions. Dark balls represent metal centres. For heteropolyanions, the black polyhedra contain the heteroatom, X.

highly charged Lindqvist anions $[Nb_6O_{19}]^{8-}$ and $[Ta_6O_{19}]^{8-}$, the experimental geometries are less well reproduced,[7] probably because the crystal field effects are great and are not taken into account in these calculations.

In the absence of paramagnetic ions, HPAs in general, and Keggin anions in particular, have a *simple* electronic structure in which the doubly occupied orbitals, formally delocalised over the oxo ligands, and the unoccupied set of d–metal orbitals are perfectly separated. In fully oxidised Keggin anions, the latter are symmetry-adapted d–metal orbitals with some antibonding participation of oxygen orbitals (Scheme 1). Because of the high

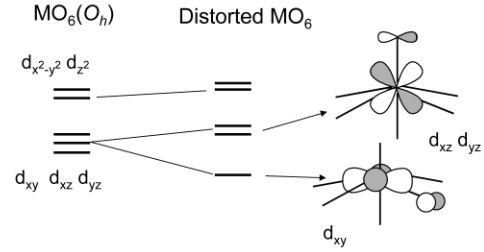

Scheme 1

oxidation state of metals in POMs, the t_{2g}-like orbitals are the most interesting in these clusters. Provided the MO_6 octahedra are distorted from the ideal O_h symmetry in Keggin anions, the d_{xy}, d_{xz} and d_{yz} orbitals are differently destabilised depending on how effective the antibonding interactions are with neighbouring p-oxygen orbitals. This overlap is more important between d_{xz} and d_{yz} with O(term) because the M–O bond lengths are shorter and the orientations are more favourable. Consequently, the LUMO in POMs are always symmetry-adapted combinations of d_{xy}-like orbitals. A 3D representation of one of the e symmetry components of both the degenerated HOMO and LUMO is given in Figure 3.

The energy gap between the occupied and the unoccupied band in Keggin anions without paramagnetic ions has been

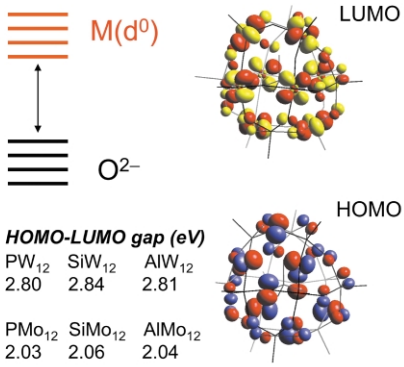

Fig. 3 Molecular orbitals scheme for a α-Keggin anion. The separation between the M and O^{2-} bands represents the HOMO-LUMO gap, listed for a series of X and M. In $[SiW_{12}O_{40}]^{4-}$ the HOMO is composed in a 95% of p–oxygen orbitals whereas the LUMO has a 73% of d–metal orbitals. 3D-representations of one e component for each MO are showed. Reproduced from ref. 9 with permission.

proven to be independent of X. Using the BP86 functional and a TZP–quality basis set for tungstates, Maestre *et al.* found a constant HOMO-LUMO gap of ~2.8 eV for different X.[9] At the same level of theory, this value decreases to 2 eV for molybdates. There is a direct relationship between the energy of the LUMO and the oxidising power of the POM. Therefore, the lesser energy of the lowest d–metal orbitals in molybdates means that they can generally be more easily reduced than tungstates to produce heteropoly blues. For example, it is well established that $SiMo_{12}$ and $GeMo_{12}$ are more powerful oxidising agents than the homologous tungstates by ~0.5 V.[1] We frequently use the terms *band of unoccupied orbitals* and *oxo band*. It is worth noting though that these sets of orbitals do not form a band in the strict sense, since the orbital energy levels remain discrete at least for the relatively small clusters discussed here.

Bridgeman and Cavigliasso described the nature of the occupied orbitals in several polyanions. Three sets of molecular energy levels are identifiable in $[M_6O_{19}]^{n-}$ Lindqvist structures: the low-lying orbitals basically composed of nonbonding combinations of s oxygen orbitals, the high-lying set composed of nonbonding combinations of p oxygen orbitals and an intermediate set that corresponds to M–O bonding interactions of essentially M(d)–O(p) character.[7] The gap between the s and p oxygen orbital sets is ~10 eV. An equivalent band structure was found for $[W_{10}O_{32}]^{4-}$[8] and other isopolyanions. In $[TeM_6O_{24}]^{6-}$ and $[PM_{12}O_{40}]^{3-}$ there is an additional level associated with the heteroatom that lies between the s and p oxo band (~7 eV above the s band).[10] Delocalised σ and π bonds along the interpenetrating M–O closed loops are considered to be a structural-stability factor of a polyanion. For the $[W_{10}O_{32}]$ framework, for instance, two types of closed loops can be considered: the twelve-membered W_6O_6 rings that are built along the *axial* direction and the eight-membered W_4O_4 rings that lie in the *equatorial* planes. σ and π out-of-plane interactions along the W_4O_4 closed loops are clearly visible in Figure 4.[8]

A measure of the relative bonding capacity and strength of the distinct oxo ligands in an isopolyanion can be obtained through the formation process of a M*x*O*y* cluster as:

$$[M_xO_{y-1}]^{(n-2)-} + O^{2-} \rightarrow [M_xO_y]^{n-}$$

The average bonding energies (ΔE_B) for terminal, bridging and central oxygen atoms in Lindqvist structures showed that the loss of an O^{2-} ligand in $[M_6O_{19}]^{2-}$ to give the neutral cluster M_6O_{18} is highly endothermic (>20 eV). ΔE_B for the bridging and terminal sites are similar although they have different bond orders according to the Mayer bond order index. ΔE_B is somewhat smaller for the central oxygen. This trend was also observed in $[W_{10}O_{34}]^{4-}$, in which the oxygen linked to five

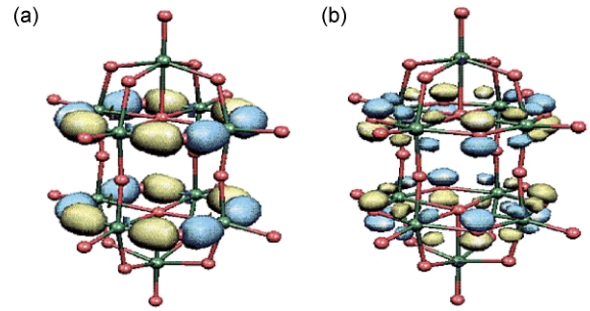

Fig. 4 3D representation of (a) σ and (b) π W_4O_4 closed loops for $[W_{10}O_{32}]^{4-}$. Reproduced from ref. 8 with permission.

metal ions is again the site with the lowest bonding energy.[8] The connection between those bonding energies and the catalytic properties of a given anion, which are frequently associated with the loss of a terminal or a bridging oxygen, would not be direct because the effects of the solvent and the relaxation of the lacunary anion were not considered.

3 Substituted clusters

Beyond the highly symmetric anions of formula $[XM_{12}O_{40}]^{n-}$, there are many clusters in which one or some $M^{n+}O_6$ octahedra have been formally replaced by another unit usually with a different metal centre like V^{5+}, Nb^{5+}, Ti^{4+}, *etc*. The distortion generated by this replacement is essentially limited to the region of substitution. Changes in the electronic structure are, however, much more important. The metal substitution modifies the energy and composition of the lowest unoccupied orbitals and, therefore, the redox properties of the molecule. Poblet and co-workers discussed this phenomenon for several mixed HPAs.[9,11] Their main conclusion is that the properties of the LUMO are quite well correlated with the electron affinity of each *isolated* M^{n+} ion, which is in the order $Mo^{6+} > V^{5+} > W^{6+} \gg Nb^{5+}$. Substituting three W ions of SiW_{12} by three Mo ions alters the relative energy of the LUMO, being 0.3 eV closer to the oxo band in A-α-SiW_9Mo_3 than in the parent single-addenda form (Figure 5). DFT calculations carried out on the

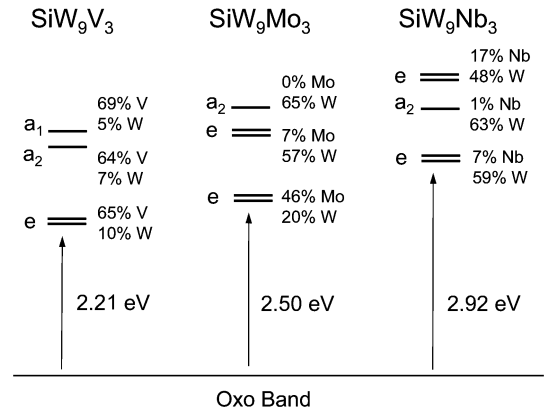

Fig. 5 Relative energies and composition of lowest unoccupied orbitals for several $[SiW_9M_3O_{40}]^{n-}$ anions. Reproduced from ref. 11 with permission.

monoreduced derivatives of α-SiW_{12} and A-α-SiW_9Mo_3 show that the first reduction is more favourable in the substituted cluster by ~0.4 eV. This value is fairly consistent with the 0.54 V obtained experimentally. Although the ionisation energies of isolated metal ions suggest that the reduction of mixed-addenda molybdovanadates should occur at the molybdenum centres, the extra electron preferentially goes to a vanadium atom. There-

fore, the reduced species $SiMo_{11}V^{IV}$ with one electron localised on the V centre is more stable than the heteropolyblue $SiMo_{11}V1e$ with one electron delocalised among the eleven Mo centres by 0.2 eV. The energy difference for the analogous tungstovanadate $SiW_{11}V$ is 0.64 eV.[9] On the other hand, Nb is more predisposed than V to lose its electrons. In agreement with this tendency, Nb orbitals have a low contribution to the lowest metal orbitals in tungstoniobate clusters, as Figure 5 shows. The heteropolyblue SiW_9Nb_31e is, therefore, the reduction product of SiW_9Nb_3.

4 Redox properties of clusters with unequivalent metal sites: the cases of $[X_2M_{18}O_{62}]^{n-}$ and $[M_{10}O_{32}]^{m-}$

After the Keggin anion $[PW_{12}O_{40}]^{3-}$, the $[P_2W_{18}O_{62}]^{6-}$ Wells–Dawson (WD) anion, P_2W_{18} in short, is one of the most common tungstophosphates. The formal substitution of three corner-sharing octahedra in α-PM_{12} by a PM_9 unit breaks the equivalence of the metal centres and gives a structure of D_{3h} symmetry that has two different metal positions, six *polar* (or cap) and twelve *equatorial* (or belt) sites (see Figure 2). Figure 6 compares the relative energies of the lowest unoccupied

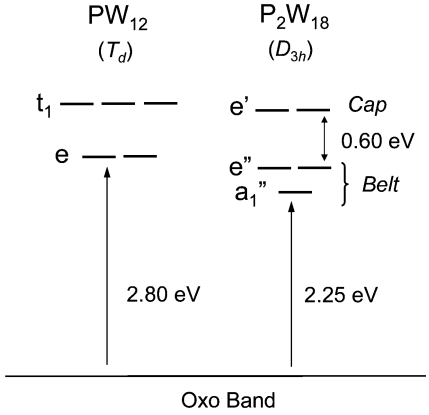

Fig. 6 Comparison of the frontier orbitals of the α-Keggin and Wells–Dawson anions. Cap and belt indicates the localisation of each MO.

orbitals in Keggin and WD structures. For single-addenda clusters, the belt metals are the major contributors to the LUMO and LUMO+1, whereas the LUMO+2 is mostly an orbital delocalised over the polar region. A direct consequence of this composition is that the first reductions in a WD anion take place at the equatorial sites. This is caused by the corner-sharing disposition of octahedra in the equatorial region, where antibonding interactions are weaker than in Keggin-like (edge-sharing) polar regions.[11] UDFT calculations carried out for the single-reduced P_2W_{18} showed that the ground state is a $^2A_1''$ with 98% of the spin density delocalised over the belt tungstens. The alternative reduction on the cap metals involves the addition of one electron to the LUMO+2 and the associated state of $^2E'$ symmetry appears 0.84 eV above the ground state. Similar behaviour was reported for the analogous P_2Mo_{18}, but the energy difference in the reduction between the cap and belt sites is slightly lower. α-P_2Mo_{18} is a chiral D_3 structure in which the Mo atoms are displaced within their respective MO_6 units, giving rise to loops of alternating short and long Mo–O–Mo bonds. This structure was well reproduced with DFT calculations, with Mo–O(brid) distances of 1.82 and 2.12 Å. The symmetry descent from D_{3h} (analogous to P_2W_{18}) to D_3 in the molybdate stabilises the cluster by more than 7 kcal mol^{-1}.

If a more electronegative ion like V^{5+} is incorporated into a polar region, an inversion of the traditional reduction order in the cap/belt sites can occur. The $P_2W_{15}V_3$ anion, in which three neighbouring cap Ws are replaced by three Vs, was studied using DFT[11] and Extended Hückel[12] calculations, showing the expected inversion. The degenerate orbital of e symmetry (e′ in the unsubstituted D_{3h} structure), centred in the polar regions, converts in the LUMO in $P_2W_{15}V_3$ (see Figure 7). According to

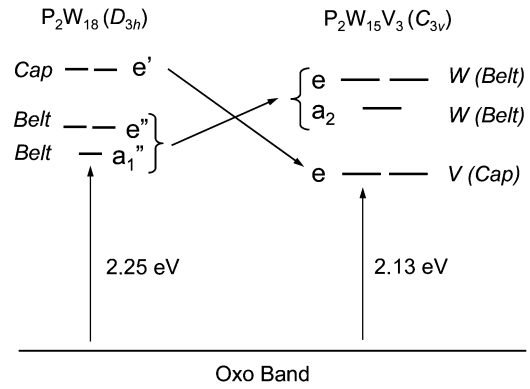

Fig. 7 Correlation diagram between the unsubstituted $[P_2W_{18}O_{62}]^{6-}$ and cap substituted $[P_2W_{15}V_3O_{62}]^{9-}$ Wells–Dawson anions.

this new ordering, the first reduction takes place at the vanadium centres and the ground state is ^2E with the spin density essentially localised on the vanadium centres. The reduction in the belt tungstens requires 0.33 eV more, according to the DFT calculations carried out by López *et al.*[11] For the analogous vanadomolybdate $P_2Mo_{15}V_3$, there is a stronger competition between the *most favourable belt site* and the *higher electronegativity* of the V^{5+} ion, since the Mo orbitals are lower in energy than those of W. Consequently, the energy difference between the two reduction sites is smaller than 5 kcal mol^{-1}.[11]

As in WD structures, the metal atoms in the decatungstate anion $[W_{10}O_{32}]^{4-}$ can also be classified as *axial* and *equatorial* centres (Figure 2). BP, BP86 and B3LYP calculations predict that the LUMO in $[W_{10}O_{32}]^{4-}$ is an orbital of a_{1u} symmetry mainly delocalised over the equatorial centres.[8] Figure 8 shows

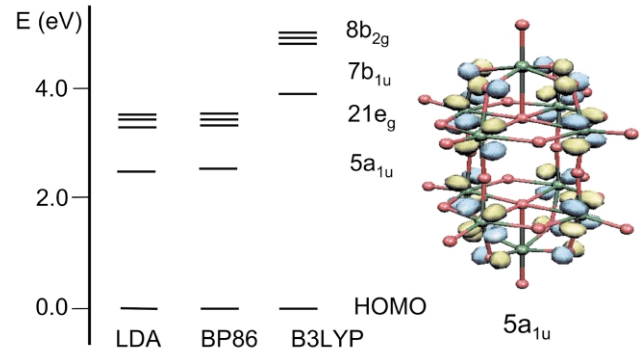

Fig. 8 Orbital diagram for $[W_{10}O_{32}]^{4-}$. Adapted from ref. 8 with permission.

orbital energies for the four lowest unoccupied orbitals and a plot of the LUMO in $[W_{10}O_{32}]^{4-}$. As expected from the composition of the LUMO, the ground states for the reduced species $[W_{10}O_{32}]^{5-}$ and $[W_{10}O_{32}]^{6-}$ are a doublet and a singlet, respectively, with the additional electrons delocalised among the equatorial sites. The diamagnetism predicted by the calculations for $[W_{10}O_{32}]^{6-}$ fully agrees with the experimental evidence. For the monoreduced species, the reduction at the axial centres (configuration $7b_{1u}^1$) was estimated to require ~1eV more than in the equatorial sites. By means of the energy decomposition scheme in terms of electrostatic interaction, Pauli repulsion and orbital mixing, Bridgeman *et al.* showed

that the equatorial-reduced states are favoured by orbital mixing and to some extent by electrostatic factors. Otherwise, the states that involve the addition of one electron to the most distant axial sites have a smaller Pauli repulsion. In other words, as Borshch suggested from Extended Hückel calculations,[13] the gain in energy due to delocalisation over the equatorial sites exceeds the loss associated with the larger electronic repulsive effects and is the factor that determines the reduction site.

5 Relative stability in α- and β-Keggin and Wells–Dawson heteropolyanions

Until the work of Weinstock and co-workers[14] on the kinetics and thermodynamics of the α/β equilibrium in Keggin tungstoaluminates, the relative instability of β isomers of Keggin anions was accepted as a general rule.[15] These authors estimated the difference in energy between the two isomers for $[AlW_{12}O_{40}]^{5-}$ in 2.1±0.5 kcal mol^{-1}. Poblet's group investigated the basis of this small difference by studying the series of Keggin anions $[XM_{12}O_{40}]^{n-}$ (M = W or Mo and X = a main group element)[16] as well as the $[P_2Mo_{18}O_{62}]^{6-}$ and $[P_2W_{15}M_3O_{62}]^{m-}$ (M = W and V) WD anions.[17] Calculations performed at DFT/BP86 level indicate that the β-Keggin anions are progressively stabilised in the order Al(III) > Si(IV) > P(V) in tungstates and molybdates.

Many POMs are considered supramolecular structures because the host and guest units are clearly distinguishable.[18] Lindqvist, Keggin and WD species have also been formulated as clathrate-like entities as $O^{2-}@[M_6O_{18}]^{(m-2)-}$, $[XO_4]^{n-}@[M_{12}O_{36}]^{(m-n)-}$ and $[XO_4]_2^{n-}@[M_{18}O_{54}]^{(m-2n)-}$. So, for example, the $[PW_{12}O_{40}]^{3-}$ Keggin anion may also be seen as a $[PO_4]^{3-}$ encapsulated by the neutral $W_{12}O_{36}$ cage. Net charges computed through Mulliken's partition for a series of HPAs confirm Day and Klemperer's hypothesis of charge localisation.[19] There is a close relationship between the total charge of the anion and the net charge on the internal XO_4 tetrahedron. When going from $[PW_{12}O_{40}]^{3-}$ to $[SiW_{12}O_{40}]^{4-}$, the net charge on XO_4 increases by 0.93e, which is almost the same change in the total charge of the cluster. This tendency is maintained for clusters with larger net charges.

The clathrate model is very useful for understanding phenomena like the α/β-Keggin relative stability. Let us take the neutral $W_{12}O_{36}$ cage. Its α form, of T_d symmetry, is 0.4 eV more stable than the β form (C_{3v}). When the phosphate anion is incorporated inside the POM, the structure of the cage contracts and the metals approach the oxygens of the PO_4^{3-} anion. The relative energy of the two cages at their respective α and β geometries, on the other hand, did not change very much. Because the energy of the internal tetrahedron is almost identical in α and β, the fragments by themselves always slightly favour the α isomer as the most stable form. This confirms the assumed greater intrinsic stability of the α organisation of d^0-metal ions and oxo ligands. López *et al.*[16] decomposed the interaction energy between XO_4^{n-} and $M_{12}O_{36}$ for a series of anions into two terms: steric repulsion and orbital interaction. The gain in stability of β when the charge of XO_4^{n-} increases was attributed to a larger polarisability of the beta cage. This conclusion is supported by a recent experimental study.[20]

β-Structures reduce at more positive potentials than the α isomers. Consequently, reduced β isomers increase their relative stability. The lowering in symmetry when going from α to β and the subsequent decrease in energy of the LUMO (Figure 9) increases the stabilisation of β when this orbital is occupied. For example, the fully oxidised α-PW_{12} is 0.28 eV more stable than the β isomer, whereas this difference is only 0.13 eV for the monoreduced pair. To understand the factors affecting the stability inversion in reduced species, López *et al.* compared the redox properties of the isolated $M_{12}O_{36}$ cage and those of the complete $XO_4^{n-}@M_{12}O_{36}$ cluster (Figure 10). The

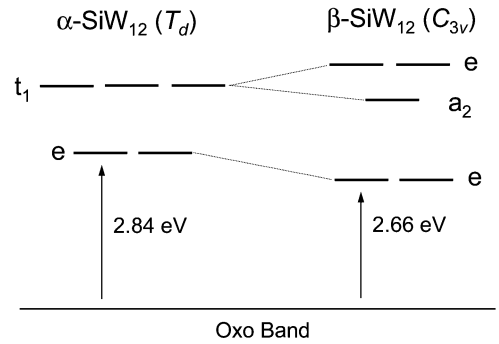

Fig. 9 Effect over the MO structure produced by the symmetry descent when an edge-sharing M_3O_{13} fragment is rotated in the α-Keggin framework of T_d symmetry to give the β form of C_{3v} symmetry. Reproduced from ref. 16 with permission.

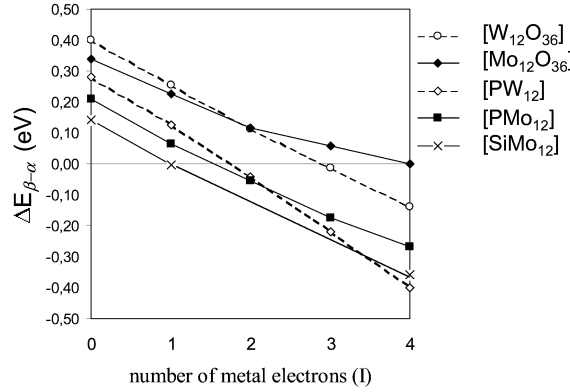

Fig. 10 Energy difference (in eV) between isomers α and β for a series of Keggin anions an $M_{12}O_{36}$ cages. Reproduced from ref. 16 with permission.

most symmetric α neutral $W_{12}O_{36}$ cage is, by 0.40 eV, initially the most stable one; after the third reduction (I = 3) both cages have similar energies, and for I = 4 the β cage is slightly more stable. When the XO_4^{n-} anion is encapsulated inside the POM, all the $\Delta E_{\beta-\alpha}$ become more negative, as is shown for the phosphate. Molybdates behave in a similar way and, in general, the α/β inversion takes place after the second reduction (I = 2).

In the WD structure (X_2M_{18}), the most symmetric α isomers are also the most stable ones; however, the energy differences are smaller than in Keggin anions. The computed energy difference of 1.83 kcal mol^{-1} between the two rotational isomers of D_{3h} and C_{3v} symmetry of P_2W_{18} is not too far from the recently reported experimental energy (3–4 kcal mol^{-1}).[21] Reduction of a WD framework also favours the less symmetric β structure, but to a lesser extent than in the Keggin framework because the 60° rotation of one M_3O_{13} unit does not significantly decrease the LUMO of the cluster.[17] Therefore, adding two electrons to the non-degenerate LUMO of P_2W_{18} hardly stabilises the less symmetric isomer, whereas the same process in the phosphotungstate Keggin anion produces a large stabilisation. For both of these species, the β isomers always reduce at more positive potentials than the α isomers but the differences are larger for Keggin structures.

6 Heteropolyanions with paramagnetic ions

Heteropolyanions may incorporate *central* or *peripheral* paramagnetic transition metal ions. The structure of a Keggin anion,

with a paramagnetic ion such as Fe^{III} or Co^{II} occupying the centre of the cluster, is not unlike those in which the heteroatom is a main group element. A direct consequence of the lack of deformation in the $M_{12}O_{36}$ cage is that the energy gap between the doubly occupied oxo band and the set of unoccupied tungsten orbitals is not modified by the paramagnetic ion in the central tetrahedron. The d-cobalt orbitals appear well separated from the oxo and tungsten band, except for the unoccupied β-t_2 orbital, which is inserted into the tungsten band (Figure 11). In

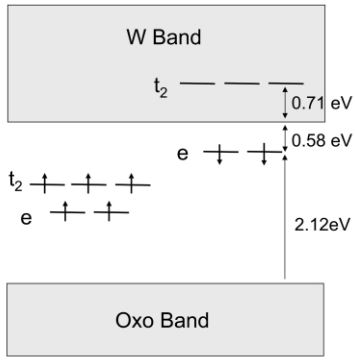

Fig. 11 Frontier orbital region for the $[Co^{II}W_{12}O_{40}]^{6-}$ anion. The t_2 and e sets of orbitals correspond to the d orbitals of Co^{II}.

open-shell systems the spin densities allow to know the localised or delocalised nature of the unpaired electrons. For $Co^{II}W_{12}$, the spin density is strongly localised in the cobalt centre but contributes little to the tetrahedral oxygens. For two other ions such as Co^{III} and Fe^{III}, the delocalisation of the spin density is somewhat higher.[9]

It is well established that the first reduction of $Co^{III}W_{12}$ takes place at the cobalt ion and produces $Co^{II}W_{12}$, whereas the subsequent reduction produces the heteropolyblue $Co^{II}W_{12}1e$ instead of $Co^{I}W_{12}$ (Scheme 2). On the other hand, the reduction

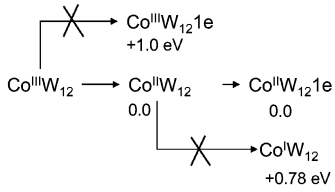

Scheme 2

of $Fe^{III}W_{12}$ leads directly to the blue species $Fe^{III}W_{12}1e$. For the ground state of $[CoW_{12}O_{40}]^{6-}$, the promotion of 1e from the highest β Co orbital to the lowest W orbital requires ~1eV. This large amount of energy explains why the blue species $Co^{III}W_{12}1e$ is not the reduction product of $Co^{III}W_{12}$ because the additional electron goes to the cobalt orbital. The subsequent reduction, however, does not occur at the cobalt centre because the blue species $Co^{II}W_{12}1e$ is 0.78 eV more stable than $Co^{I}W_{12}$. This is a product that requires the addition of one electron to the β-t_2 orbital, which is 0.71 eV above the lowest unoccupied tungsten orbital.

The unrestricted DFT energies computed for an open-shell configuration represent an average of the individual multiplets associated with a given configuration. The energy of a particular multiplet can be formulated as the weighted sum of single determinant energies. With the aid of the STAGEN program for determining the symmetry coefficients for wave functions and energies,[22] Maestre *et al.* computed the multiplet splittings for several excited configurations of $[Co^{II}W_{12}O_{40}]^{6-}$.[23] For the excited $e^3t_2^4$ configuration there are two quadruplets of symmetries $T_2(F)$ and $T_1(F)$ that are at 7126 and 13711 cm^{-1} above the $^4A_2$ ground state, which is associated with the ground configuration $e^4t_2^3$. These energies are too large if we compare them with the assignments made for the permitted Co → Co transition $^4A_2 \rightarrow {}^4T_1$ (7830 cm^{-1}) and the forbidden transition $^4A_2 \rightarrow {}^4T_2$ (4600 cm^{-1}). There is strong agreement when a Jahn–Teller relaxation is permitted for the excited configurations. The states $^4T_1$ and $^4T_2$ in the T_d geometry split into the four states $^4B_2$, $^4E(2)$ and $^4A_2$ in the D_{2d} geometry. As Figure 12

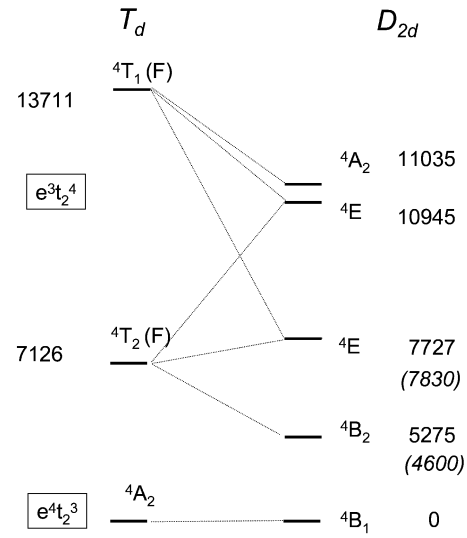

Fig. 12 Multiplet splitting (in cm^{-1}) for the excited configurations $e^3t_2^4$ of $[Co^{II}W_{12}O_{40}]^{6-}$ in the D_{2d} symmetry. The values in parentheses correspond to the experimental transition energies. Reproduced from ref. 23 with permission.

shows, the lowest state of symmetry B_2 appears at 5275 cm^{-1}, a value that agrees fairly well with the energy expected for the forbidden transition $^4A_2 \rightarrow {}^4T_2$. The energies of the next excited states range between 7700 and 11000 cm^{-1}. These values agree well with the presence of an intense, broad band in the near-infrared region (7000–9000 cm^{-1}) in the electronic spectrum of $[Co^{II}W_{12}O_{40}]^{6-}$. Superposed to the Co → Co transitions are charge-transfer transitions from Co to W.

Substituting addenda metal atoms by paramagnetic ions provides highly interesting clusters. Derivatives containing Mo and Fe are one example. The closeness of the redox potentials for Mo^{VI}/Mo^{V} and Fe^{III}/Fe^{II} in oxides allows the equilibrium

$$Fe^{II} + Mo^{VI} \rightarrow Fe^{III} + Mo^{V}$$

when both ions are in octahedral sites. Duclusaud and Borshch studied this process[24] in the Keggin framework through a model cluster including only the region of Fe and two neighbouring Mo atoms. Two minima that differ by less than 1 kcal mol^{-1} were found at the B3LYP level, corresponding to the one-electron-transfer between Fe and Mo. Figure 13 shows the two

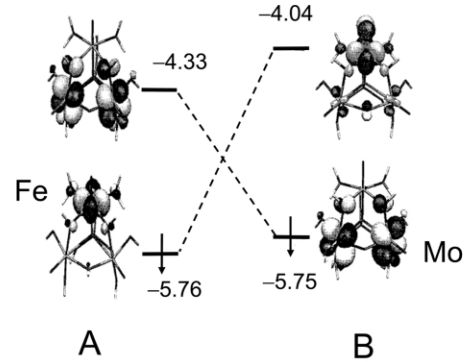

Fig. 13 Molecular orbitals involved in the electronic transfer between iron and molybdenum orbitals in an iron-substituted Keggin cluster (energies are in eV). Reproduced from ref. 24 with permission.

orbitals involved in this transfer. Minimum A represents the situation in which all metal electrons are at the iron centre with

a high-spin configuration, $t_2^4e^2$, and with one β-electron in the orbital. Minimum B represents the situation in which this β-electron has been transferred to a molybdenum orbital. The only noticeable difference between the geometries of A and B is the coordination sphere around Fe, which is more contracted in B. The small energy difference between the two localisation patterns and the probable absence of an energy barrier between them suggest fast electronic transfer between the two metals at room temperature. This would agree with the interpretation of the Mössbauer spectra for this sort of system.[24] A similar model was used to describe the electron transfer between a Keggin unit and an Fe counterion.[25]

7 Magnetic properties of reduced anions

7.1 Magnetism modulated by substitution

POMs are versatile building blocks for constructing molecular magnetic materials. Many POM-based materials present the coexistence of localised and delocalised magnetic electrons. Duclusaud *et al.*[26] evaluated by means of Broken Symmetry procedure at DFT level how the magnetism of the nitrosyl derivative of the decamolybdate ion, $[Mo_{10}O_{25}(OMe)_6(NO)]^-$, is affected by the position of the six methoxy ligands. The structure of this anion is related to that of $[Mo_{10}O_{34}]^{4-}$ (Figure 2) and may be viewed as a $Mo_{10}O_{34}$ framework in which one terminal oxygen is replaced by a NO group and six bridging oxygens are replaced by six methoxy groups. By modelling the CH_3 groups with H atoms, the five isomers represented in Figure 14 were studied. As in $[W_{10}O_{34}]^{4-}$, the LUMO for the

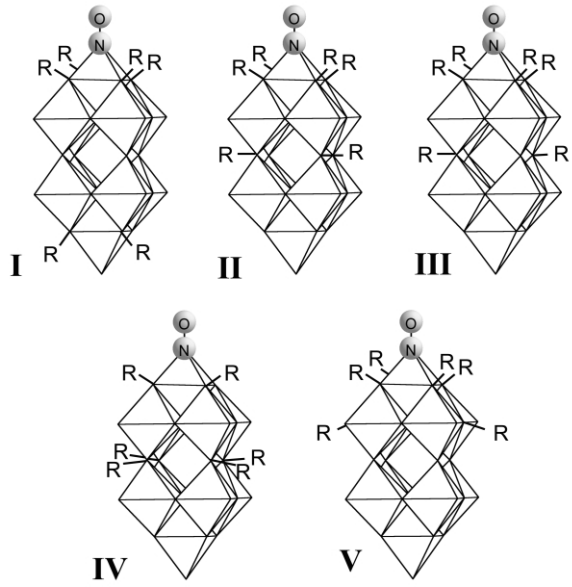

Fig. 14 The five isomers studied for $[Mo_{10}O_{25}(OMe)_6(NO)]^-$. R represents the methoxy group and was modelled by H in the calculations.

fully oxidised parent of **I** ($[Mo_{10}O_{25}(OMe)_6(NO)]^+$ is an orbital delocalised over the eight equatorial Mo ions, and well separated from the next unoccupied level. Consequently, the two additional electrons are accommodated in the LUMO, which gives rise to a diamagnetic ground state for $[Mo_{10}O_{25}(OMe)_6(NO)]^-$. We could modify the diamagnetism of this anion if we could reduce the HOMO-LUMO gap and get an open-shell state (triplet or singlet competitive with the closed-shell configuration). Since the HOMO in $[Mo_{10}O_{25}(OMe)_6(NO)]^-$ is localised on the eight equatorial molybdenum ions, we expect the protonation in the bridging oxygens of the equatorial planes or between the equatorial planes to alter the energy of the HOMO and its separation with respect to the LUMO. In isomers **II** and **III**, two of the four bridging oxygen sites that link the two equatorial planes are protonated. The ground state in the two structures is a singlet closed-shell, but it is worth noting that the HOMO-LUMO gap is reduced from 1.09 (**I**) to 0.90 (**II**) and to 0.66 eV (**III**) when a BP86 functional is used. If all four bridging oxygen atoms that connect the two equatorial planes are protonated (isomer **IV**), the frontier orbitals get closer in energy 0.55 eV. Finally, isomer **V** represents a situation with two protonated equatorial-bridging oxygens.

It is well known that DFT functionals overestimate electron delocalisation and that the best magnetic coupling constants are obtained with the hybrid B3LYP functional. With this functional and using LDA geometries, the energy gap between the singlet closed-shell and the triplet state was estimated for isomers **I**, **II** and **III**. All these isomers have the triplet above the singlet, but their relative energies decreases from 0.6 eV in **I** to 0.18 eV in **III**. In **IV**, the ground state is the triplet state at only 0.0027 eV from the singlet. The latter state was computed with the Broken-Symmetry approach. Indeed, this solution is lower than the triplet state in isomer **V**, with a difference of 0.001 eV. To sum up, Duclusaud and Borshch have proven that the magnetic properties of a reduced cluster can be conveniently tuned by controlling the position of a substituent in POMs.

7.2 *Ab initio* determination of electron-transfer parameters in reduced Keggin anions

Experimentally, it is well established that when Keggin anions contain an even number of delocalised electrons the compound is diamagnetic. Initially, this phenomenon was attributed to a strong antiferromagnetic coupling *via* a superexchange mechanism.[27] It was later shown through model calculations that electron delocalisation and electron repulsion can stabilise the diamagnetic singlet.[28] Coronado and coworkers recently reported very accurate *ab initio* calculations to evaluate electron-transfer parameters in reduced Keggin anions.[29] Provided the transfer (hopping) effective integrals are essentially local parameters, fragments can properly model the Keggin framework. These authors used 4W- and 2W-ion fragments (Figure 15) to estimate transfer integrals in the one-electron-reduced cluster. Taking into account that the unpaired electrons are delocalised over d_{xy}-like orbitals of W ions, the following four doublets can be defined for the one-electron-reduced 4W-ion fragment,

$$\psi_1 = \frac{d_1 + d_2 + d_3 + d_4}{2} \quad \psi_2 = \frac{d_1 - d_2 - d_3 + d_4}{2}$$
$$\psi_3 = \frac{d_1 + d_2 - d_3 - d_4}{2} \quad \psi_4 = \frac{d_1 - d_2 + d_3 - d_4}{2} \qquad (1)$$

where d_i are the Slater determinants constructed when the extra electron is on the corresponding W_i ions. In this context, the transfer parameters t (hopping between corner-sharing WO_6 octahedra) and t' (hopping between edge-sharing WO_6 octahedra) are then written as:

$$t = \langle d_1|H|d_4\rangle \; t' = \langle d_1|H|d_2\rangle$$

These integrals are related to the doublet energies E_1–E_4 by the equations,

$$E_4 - E_1 = -2t - 2t' \; E_3 - E_2 = -2t + 2t'$$

By precisely determining the E_i energies the values obtained for t and t' are also very accurate. Contrarily to what is commonly accepted, the electron transfer between edge-sharing and corner-sharing WO_6 octahedra was very similar for all methods and fragments used. For the largest fragment, the most accurate calculation was performed at the CASPT2 level, giving

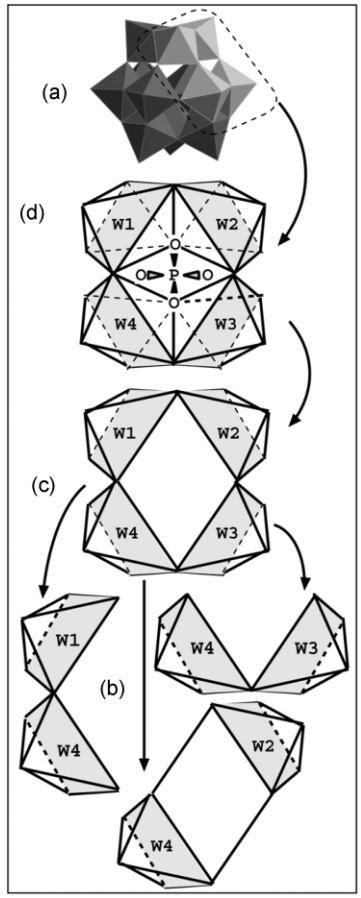

Fig. 15 (a) Polyhedral representation for a Keggin anion. (b)–(d) Fragments used to compute transfer (hopping) integrals. Reproduced from ref. 29 with permission.

a value of −428 meV for t and −470 meV for t'. The computed values at the same level of accuracy did not differ very much when the smallest 2W-based fragments of Figure 15d were used. For these smaller clusters, t and t' integrals were also calculated with the variational DDCI method, leading to t = −467 meV and t' = −507 meV. When the latter values were introduced into an extended Hubbard Hamiltonian,[29] the singlet state for a two-electron-reduced Keggin anion was estimated to be 280 meV more stable than the lowest triplet state. This large energy gap clearly explains the diamagnetism of the two-electron-reduced Keggin anions.

8 Localisation/delocalisation of the metal electrons in mixed polyoxoanions

Most POMs comprising metal ions in a high oxidation state can be easily reduced without making significant structural changes. It is difficult to unequivocally characterise the number and nature of the reduced centres in a partly reduced cluster and today this is still a matter of debate. Electrochemical reductions and EPR spectroscopy have usually been used to determine the localisation, or delocalisation, of the metal electrons in reduced HPAs. The intense blue colour in reduced POMs is considered to indicate an important delocalisation of the metal electrons.

As we have mentioned above, the monoreduction of the mixed $SiVW_{11}$ anion yields the brown species $SiV^{IV}W_{11}$, not the heteropoly blue, $SiVW_{11}1e$. The first two electrochemical reductions in $SiMoV_2W_9$ and the first three electrochemical reductions in SiV_3W_9 were attributed to $V^V \rightarrow V^{IV}$ steps.[30] Through empirical valence sum calculations based on the X-ray structure of the highly reduced bicapped Keggin complex $[PMo_{12}O_{40}(VO)_2]^{5-}$, two of the eight d electrons were assigned to the two V centres and the other six electrons were considered to be delocalised among the other 12 Mo centres.[31] This distribution was fully confirmed by DFT calculations, which showed that the ground state was a triplet with two V^{IV} ions.[32] The alternative configuration, corresponding to an equipartition of the eight electrons between vanadium and molybdenum centres, was less stable by 1.41 eV. Xu *et al*. synthesised the related tetracapped cluster $[Mo_8V_8O_{40}(PO_4)]^{5-}$ as an anion with eight V^{IV} centres with the other two d electrons delocalised over the eight Mo atoms.[33] When then number of vanadium ions increases, the hypothesis that before accommodating any electron in a Mo orbital all vanadium centres should have at least one electron does not seem to be satisfied. Preliminary calculations carried out by our group on $[Mo_8V_8O_{40}(PO_4)]^{5-}$ indicate that the configuration with eight electrons on the 8 V centres and the two remaining electrons on the 8 Mo atoms is much more unstable than the more equilibrated repartition of the electrons, *i.e*. six electrons over the V centres and the other four electrons over the Mo centres.

Using DFT/BP86 calculations, Rohmer and Bénard discussed the nature of the M–M bond in the two-reduced oxothio clusters γ-$[SiW_{10}M_2S_2O_{38}]^{6-}$ (M = Mo, W) recently synthesised by Cadot and Sécheresse.[34] The X-ray characterisation of these structures revealed short M^V–M^V distances (2.832 Å for M = Mo and 2.815 Å for M = W). These values clearly indicate that Mo–Mo and W–W are single bonds (Figure 16).

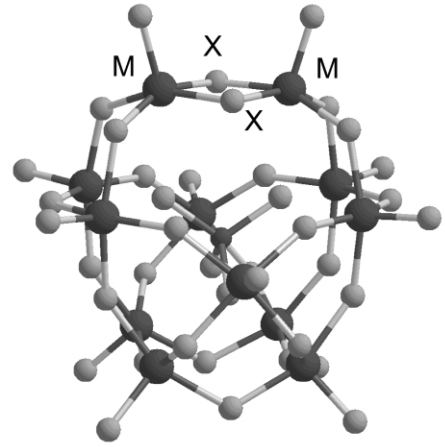

Fig. 16 Ball and stick representation for the γ-$[SiW_{10}M_2X_2O_{38}]^{6-}$ anion (M = Mo, W and X = O, S).

The oxoanions γ-$[SiW_{10}Mo_2O_{40}]^{6-}$ and γ-$[SiW_{12}O_{40}]^{6-}$ were also synthesised but could not be characterised crystallographically. For the four anions a first minimum with a short M–M separation was found. The computed M–M separations in the oxothio anions, 2.998 Å for M = Mo and 2.872 Å for M = W, were somewhat longer than the distances observed but these structures maintained the presence of a metal–metal coupling. The corresponding metal–metal distances for the oxo anions were 2.653 and 2.569 Å. All the complexes have similar electronic structures, an occupied valence O/S band that is well separated from the empty d–Mo/W band and an isolated HOMO localised on the $M_2X_2O_2$ fragment that is typical of a σ_{M-M} bond (Scheme 3). A new minimum characterised by a long M–M distance (> 3 Å for X = O and > 3.7 Å for X = S) and with the two electrons delocalised over the γ-Keggin tungstate was reported. Except for γ-$[SiW_{12}O_{40}]^{6-}$, the most stable conformation is the one with the short metal–metal distance, with energies ranging from 10.2 to 23.8 kcal mol^{-1}. In the unsubstituted tungstate, the delocalised state is lower in energy by 2.9 kcal mol^{-1} This seems to be consistent with the blue colour of the anion in solution. The other three anions are red or

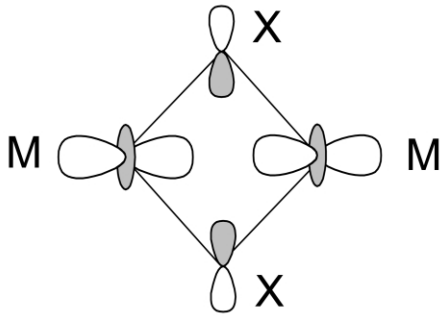

Scheme 3

red-brown. The localisation/delocalisation of the two metal electrons in the γ-$[SiW_{10}M_2X_2O_{38}]^{6-}$ clusters therefore depends on the difference between the electrophilic characters of the Keggin core, γ-$[SiW_{10}O_{36}]^{n-}$, and the flexible dimetallic fragment, $M_2X_2O_2$.[34]

9 Proton affinity of polyoxoanions

Heteropoly acids are considered to be significantly stronger than typical inorganic acids such as H_2SO_4, HNO_3, HCl, *etc*. The negative charge of HPAs, which are larger than inorganic acids, is delocalised among a large number of oxygen sites, so the electrostatic interactions between the proton and the anion are weaker. In general, heteropolytungstates are more acidic than molybdates, whereas the effect of the heteroatom is less important. The order of acid strength for some heteropoly acids is $H_3PW_{12}O_{40} > H_4SiW_{12}O_{40} > H_4GeW_{12}O_{40} > H_6P_2W_{16}O_{62}$ and $H_3PW_{12}O_{40} > H_3PMo_{12}O_{40}$. Davis and co-workers[35] evaluated the acidity of $H_3PW_{12}O_{40} > H_3PMo_{12}O_{40}$ by calculating the proton affinity from the process $H_3PM_{12}O_{40} \rightarrow H_2PM_{12}O_{40}^- + H^+$. The protons in $H_3PM_{12}O_{40}$ were placed at bridging positions far away from one another. The cluster energies were computed after the complete optimisation of the diprotonated and triprotonated species. The value of 1126 kJ mol^{-1} for the third bridging site in the phosphomolybdate was 38 kJ mol^{-1} larger than the proton affinity found for the tungstate. These results are fully consistent with the larger acidity of tungstates.

The first attempt to classify the basicity of the various oxygen sites in a POM was reported by Bénard and coworkers at the beginning of the 1990's.[36] The decavanadate ion $[V_{10}O_{28}]^{6-}$ offered an excellent opportunity to compare the basicity of terminal (OV), double-bridging (OV_2) and triple-bridging (OV_3) oxygen sites in the same molecule. ^{17}O NMR spectroscopy for protonated and unprotonated species suggested that sites B and C (Figure 17) were the preferred protonation sites. This was confirmed by the crystallographic characterisation of the dimeric species $[H_3V_{10}O_{28}]^{6-}$. At that time, directly determining the protonation energy for a relatively large molecule like decavanadate was unaffordable and Bénard's group discussed the local basicity of a particular site by computing the distribution of Molecular Electrostatic Potentials (MEP). Electrophilic species tend to minimise their potential energy by approaching a minimum MEP value as much as possible. The MEP distribution computed for the 26 external oxygen sites characterised 20 local minima, which were identified as probable protonation sites. The deepest ones were associated with the four triple-bridging oxygen sites B. Double bridging oxygens C and D were found at relative depths of 10 and 23 kcal mol^{-1}, respectively. According to this MEP distribution, the proton fixation preferentially takes place at the triple coordinated oxygens. The second preferred site is C and the protonation at O(term) is completely unexpected since the deepest minima in the vicinity of a terminal site appeared more

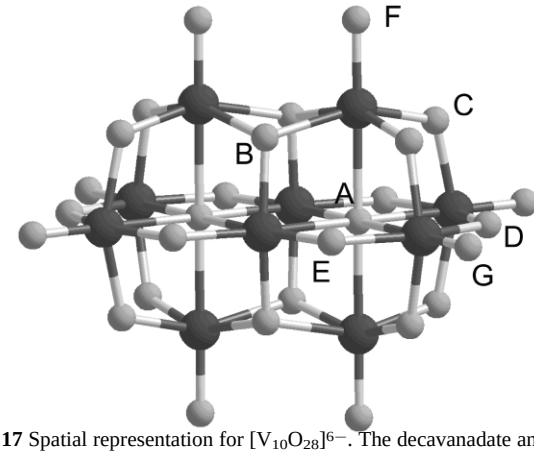

Fig. 17 Spatial representation for $[V_{10}O_{28}]^{6-}$. The decavanadate anion has six distinct oxygen sites: one OV_3 (B), three OV_2 (C, D and E) and two OV (F, G).

than 55 kcal mol^{-1} above the minimum close to site B. More recently, López *et al.* discussed the proton affinity in a series of mixed-addenda Keggin anions, SiW_9M_3 (M = Mo and V). Figure 18 shows two views of the EP distribution on a 3D-

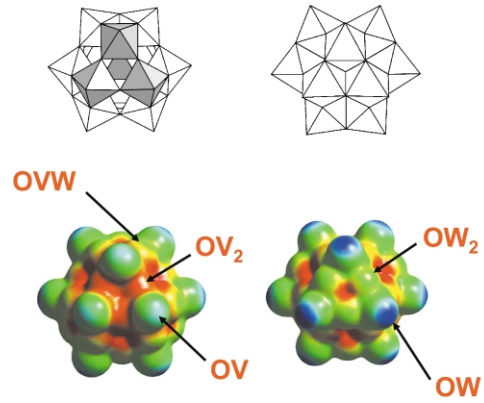

Fig. 18 Molecular electrostatic potentials for the A-α-SiW_9V_3 Keggin anion from two viewpoints. Red regions identify nucleophilic areas whereas blue regions electrophilic areas.

density isosurface. The red areas identify regions with negative electrostatic potentials (nucleophilic sites) and the blue areas identify regions of positive or less negative electrostatic potentials. A simple analysis of these MEP representations suggests that the preferred protonation site corresponds to a bridging O bonded to two Mo centres in SiW_9Mo_3 and to two Vs in SiW_9V_3. Like in decavanadate the terminal oxygens are the least nucleophilic sites. From the relative protonation energies obtained the following basicity scale was proposed: $OV_2 > OMo_2 > OW_2 > OV > OW > OM$.[11]

Amoureux and co-workers[37] used BP86 functional and a TZP-quality basis set to study the basicity of single-addenda PM_{12} anions (M = Mo, W). As expected, the protonation in the bridging oxygen sites was preferred. Protonations at terminal (O_t) oxygen were less favoured by 11.5 and 18.4 kcal mol^{-1} for PMo_{12} and PW_{12}, respectively. These values were compared with Rotational Echo Double Resonance (REDOR) NMR data, which detected the protons in $H_3PMo_{12}O_{40}$ and $H_3PW_{12}O_{40}$ at a distance of 5.20 ± 0.20 Å and 5.70 ± 0.20 Å from the central phosphorus, respectively. Both experimental values were rather larger, especially the latter. This seems only consistent with a protonation at a terminal site in H_3PW_{12}. For the first time, the general assumption that the protonation at a terminal oxygen site is only competitive in systems containing Nb, Ti or Cr was called into question. In our opinion, these results are very important because, if confirmed in other systems, they may indicate that solvent and counterions need to be considered to find the local active sites in a POM.

10 Inclusion complexes and host–guest interactions

In a series of papers, Bénard's group analysed the electronic properties of inclusion complexes such as $RCN\subset(V_{10}O_{32})^{4-}$ and electronically inverse systems in which negatively charged species are encapsulated into negatively charged anions. These studies[38–39] have recently been reviewed at length.[40] Figure 19 shows an inclusion complex characterised by the penetration of

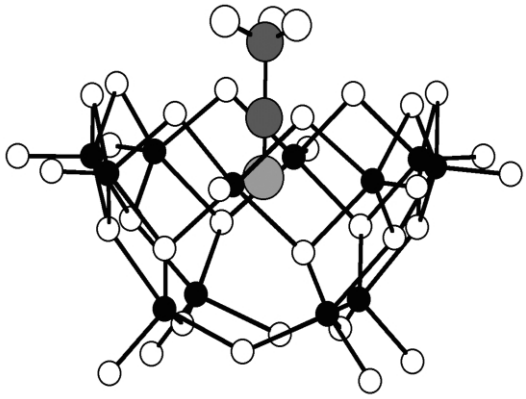

Fig. 19 The inclusion complex $CH_3CN\subset[V_{12}O_{33}]^{4-}$.

a nitrile in the hemisphere of a dodecavanadate anion.[41] For the acetonitrile complex, the experimental distance between the nitrile nitrogen and the plane that contains the four vanadium atoms at the bottom of the POM is 2.22 Å. The host–guest interaction between the two subunits remains in solution. The Hartree–Fock stabilisation energies for three R–CN guest molecules (R = H, CH_3 and C_6H_5) were found to have similar energies ranging from −12.8 to −14.4 kcal mol^{-1}.

A first analysis of the interaction between the host and guest molecules can be obtained from the molecular electrostatic potentials distributions of the two separate units. The MEP distribution for the $[V_{12}O_{32}]^{4-}$ cavity showed a saddle point that connects two regions of low potential, one in the bottom of the anion and the other more external. The upper minimum and the saddle point generate a dipolar moment that opposes that of the isolated guest nitrile. The weak stabilising interaction between N_2 and the host vanadate (−5 kcal mol^{-1}) emphasises the importance of a permanent dipole moment in the guest molecule. By superposing the MEP distributions for the host and guest subsystems, the potential minimum facing the N atom in C_6H_5CN coincided exactly with the saddle point in the host cavity. This means that the bonding between the two units follows a *lock* and *key* mechanism in which, as well as the coupling between the two opposing dipole moments, there is an electrostatic interaction between the nitrogen lone pair and the electrophilic region inside the cage. The absence of both a permanent dipole moment and a lone pair makes C_2H_2 strongly repulsive toward the $[V_{12}O_{32}]^{4-}$ cavity, since its interaction energy was found to be +10.6 kcal mol^{-1}.

By decomposing the stabilisation energy using the CSOV method, the bonding in the two observed inclusion complexes $RCN\subset(V_{10}O_{32})^{4-}$ (R = CH_3 and C_6H_5) and the model system $HCN\subset(V_{10}O_{32})^{4-}$ could be compared. For HCN and CH_3CN, the Steric term, which contains the Pauli repulsion and the Coulombic attraction, is dominated by the attractive interaction between host and guest units for both R = H and CH_3. When the size of R increases, the Pauli repulsion between the substituent R and the anion increases and the Steric term becomes slightly positive. On the other hand, the guest polarisation and the charge transfer terms are larger for R = C_6H_5, which generally produces similar interaction energies for the three substituents.[38–39]

11 Stabilising fields generated by solvent molecules and counterions

11.1 Anions in solution

Highly negative species like POMs only exist in condensed phases, where the external field generated by the solvent molecules or the counterions stabilise the anion. The instability of an *isolated* polyanion is manifested in the high energy of all its molecular orbitals. Consider $[PW_{12}O_{40}]^{3-}$ as an example and reformulate it as $PO_4^{n-}@W_{12}O_{36}$ according to the clathrate model. The LUMO in the neutral α-$W_{12}O_{36}$ cage appears at very negative energies using a BP86 functional and a Slater-type TZP basis set. When the cage encapsulates the anion $[PO_4]^{3-}$, all the orbitals are upshifted by more than 9 eV and the LUMO level lies at a positive energy. If the encapsulated anion is $[SiO_4]^{4-}$, the energy of the lowest unoccupied orbital is still higher. It is important to remember that the HOMO-LUMO gap is hardly altered by the encapsulation of the anion and that, in practice, it is independent of the central heteroatom even when it is a paramagnetic ion. Taking into account that POMs are easily reducible species, the energy of the LUMO has to be low enough to accept the incoming electron. Solvent molecules and counterions generate a stabilising field, which lowers the energy of all molecular orbitals. The continuum model of a solvent, as implemented in the COSMO program, was used to analyse the effect over Keggin and WD anions. There is a considerable stabilisation of the molecular orbitals after solvation and this magnitude parallels the net charge of the polyanion. For $[PW_{12}O_{40}]^{3-}$, the energy of the LUMO drops from +2.85 eV in the gas phase to −4.18 eV in water solution. For the most charged $[P_2W_{18}O_{62}]^{6-}$ WD anion, the LUMO in the isolated anion is very high in energy (above 8 eV at the same level of theory) and after solvation it is at −4.48 eV, which is even lower than in $[PW_{12}O_{40}]^{3-}$. This makes the process $[PW_{12}1e]^{4-} + [P_2W_{18}]^{6-} \rightarrow [PW_{12}]^{3-} + [P_2W_{18}1e]^{7-}$, which is strongly endothermic in the gas phase, slightly exothermic in water solution. In other words, the *blue* electron in the gas phase simply prefers to reside in the less charged anion. On the other hand, the metal electron prefers to stay in the WD framework after water solvation, since the LUMO is slightly more stabilised.

11.2 Modelling the crystal field

Bénard[40] proposed the following procedure to incorporate the effect of the crystal field in quantum chemistry calculations of polyoxoanions:

1. Model the surrounding crystal by a set of point charges that can be determined from a Mulliken partition or from similar procedures.

2. Determine the electrostatic potential generated at the centre of the polyanion by the point charges contained in successive shells of ions until convergence.

3. Define a uniformly charged sphere of 20 Å in diameter, centred on the target anion and with a charge that is fitted to reproduce the potential obtained in the previous step.

4. Carry out a new quantum chemistry calculation with the presence of the charged sphere.

Using this procedure the stabilisation of guest anions inside negatively charged cages was analysed. Typical examples of these electronically inverse host–guest complexes are $Cl@[H_4V_{18}O_{42}]^{9-}$ and $Cl@[V_7O_{12}(O_3PR)_6]^{2-}$, clusters, in which a halogen is encapsulated by the two anionic cages $[H_4V_{18}O_{42}]^{8-}$ and $[V_7O_{12}(O_3PR)_6]^{-}$. In agreement with the high negative charge of $[H_4V_{18}O_{42}]^{8-}$, the electrostatic potential at the centre of the cage is very negative and consequently the encapsulation of an anion has associated a very repulsive interaction between the host and the guest, which makes the

encapsulation process of the *isolated* cage non-viable. For the non-protonated model complex $[V_{18}O_{42}]^{12-}$, the electrostatic potential is still more negative. In the less charged cage $[V_7O_{12}(O_3PR)_6]^-$, the potential at the centre of the cavity is positive and therefore attractive towards a negative charge. These results for the electrostatic potential of the isolated cage can explain the formation of the $Cl@[V_7O_{12}(O_3PR)_6]^{2-}$ complex but do not allow to rationalise the encapsulation of a halogen by a highly charged hollow cage like $[H_4V_{18}O_{42}]^{8-}$. Clearly, the crystal field is needed to achieve the stability of the encapsulation cluster. Bénard and coworkers estimated the lattice potential for $Cs_9(Cl@H_4V_{18}O_{42})$ and showed that it is *positive* at the centre of the cavity, thus overcoming the negative potential generated by the anionic host. An ample review of this subject can be found in reference 40.

One of the most important limitations when determining the lattice field is the disorder in many of the crystals that contain a polyoxoanion. The crystal structure for the salt $(Et_3H)_5(PMo_{12}O_{40}(VO)_2)$ was well solved and the potential due to the crystal could be estimated. The anion $[PMo_{12}O_{40}(VO)_2]^{5-}$ has 8 metal electrons and, unlike an oxidised cluster, this highly reduced system does not need a negative charge to complete the valence shell of oxo ligands. The $[PMo_{12}O_{40}(VO)_2]$ framework, with two VO units capping a Keggin structure, has a high tendency to be negatively charged, even at the gas phase. As Figure 20 shows, the total energy of the cluster exhibits a

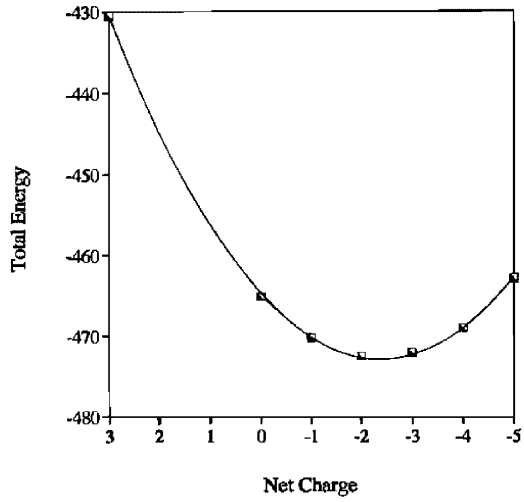

Fig. 20 Total energy of the bicapped $[PMo_{12}O_{40}(VO)_2]^{n-}$ cluster energy as a function of the net charge of the system. Reproduced from ref. 32 with permission.

minimum when the net charge of the anion is −2 and −3. These values correspond to a number of 5 and 6 metal electrons over the metal ions, respectively. This means that the $Mo_{12}V_2$ cage has a high propensity to be negatively charged. However, the isolated cage cannot reproduce the optimal number of metal electrons in the cluster (8). The counterions generate a stabilising field that increases the intrinsic tendency of the cluster to accept electrons: eight are accommodated on the d-metal orbitals.

12 Vibrational frequencies in Lindqvist and Keggin anions

The theoretical determination of vibrational frequencies for large molecules is still a non-standard task. In the case of Keggin anions, the calculation of the second derivatives of the energy is extremely computationally demanding despite their tetrahedral symmetry. In a significant study, Bridgeman computed, classified and compared the vibrational frequencies for the series of Keggin anions $[XMo_{12}O_{40}]^{n-}$, X = P^{III}, As^{III}, Si^{IV}, Ge^{IV}, Al^{V} and Ga^{V} and $[PW_{12}O_{40}]^{3-}$ using the B3LYP hybrid functional.[42] We will not describe here the 153 normal modes of vibration of an α-Keggin anion but we should point out that the B3LYP functional with augmented LANL2DZ basis sets reproduces the experimental spectrum of Keggin anions very well. The discrepancy between the calculated and the observed spectra does not exceed a few cm^{-1} for most vibrational modes. For $[PW_{12}O_{40}]^{3-}$, the largest deviation of 71 cm^{-1} takes place in a vibrational mode assigned as a combined stretching and bending Mo–O–Mo mode. Previously, the same group compared the vibrational spectra of various Lindqvist anions at several computational levels. Although DF methods reproduce the vibrational spectral of $[M_6O_{19}]^{n-}$ clusters quite well, the Hartree–Fock method performs very poorly.[43] The fitting between experimental and theoretical spectra was best at the LDA level with the TZP/ZORA approach (triple-ζ Slater basis set with the ZORA method). In comparison, the LDA and B3LYP functionals with GTO basis provide less accurate results. The results with BP86 and BLYP are significantly poorer.[43]

13 Epilogue

On assignment from various U.S. Federal Agencies, between 1999 and 2001 several scientists evaluated how molecularly-based modelling is being applied all over the world in commercial, academic and government organisations. The final report†, which was published in 2002, identified three major successful areas. These were drug discovery, homogeneous catalysis and computational thermochemistry. Among other conclusions, the authors of that report stated that: *"In the next ten years, molecularly-based modelling will profoundly affect how chemistry, biology, and materials physics are understood, communicated, and transformed to technology, both intellectually and in commercial applications"*.

Compared to other fields, the application of quantum chemistry methods to polyoxoanions is less developed. This is mainly because the theoretical treatment of such species must take into account several intrinsic difficulties. POMs are transition metal-based compounds, which are often highly charged anionic species that can exhibit open-shell electronic states and usually display multiple shapes. The work of Bénard on the decavanadate, $[V_{10}O_{28}]^{6-}$, published in the early 1990's, in which he classified the relative basicity of external oxygen sites, pioneered the application of computational methods to POMs. Since then, the continuing advances in computational power, the evolution of the quantum chemistry software and the wide acceptance by the scientific community of density functional methods have enabled other topics and more sophisticated structures to be studied.

However, the process has only just begun and POM chemistry offers great challenges. To date, most quantum chemical studies have considered anions in the gas phase, but POMs only exist in solution, or in solid state stabilised by the field that is generated by the solvent molecules and counterions. This crude representation has provided invaluable information about the relative properties of POMs, but to determine absolute values—or to compare anions with different charges—we need to consider the secondary structure. This therefore needs to be properly described if we are to make progress in the modelling of such clusters. Polyoxoanions can be giant molecules. Some of them comprise more than 150 metal ions and about 500 oxygen atoms.[18] The proper theoretical description of this piece of solids is another big challenge for the next years. DFT-based methods have helped us to understand the electronic structure of

† http//www.wtec.org/molmodel/mm_final.pdf

POMs with paramagnetic ions, but for a rigorous analysis we need to use classical multiconfigurational *ab initio* methods that today can only be applied to the smallest structures like Lindqvist $[M_6O_{19}]^{n-}$ or Anderson $[XM_6O_{24}]^{m-}$ anions. In summary, the modelling of polyoxometalate chemistry will require contributions from specialists in a number of fields including molecular dynamics, multiconfigurational quantum chemistry methods and magnetism.

Acknowledgements

This work was supported by the DGYCIT (BQU2002–04110-C02–01) and the CIRIT (SGR01–00315). We thank Professor Eugenio Coronado and Dr Adam Bridgeman for providing us with copies of their work prior to publication. We especially thank Professor Marc Bénard for introducing us into the field of polyoxometalates and for giving us support and encouragement over the years. The authors are grateful to the referees for their suggestions and comments.

References

1 See, for example: M. T. Pope, *Heteropoly and Isopoly Oxometalates*, Springer-Verlag, Berlin. 1983, page 26.
2 C. L. Hill, ed., *Chem. Rev.*, 1998, **98**, 390 (special issue on Polyoxometalates).
3 M. T. Pope and A. Müller, *Angew. Chem., Int. Ed. Eng.*, 1991, **30**, 34.
4 D. E. Katsoulis, *Chem. Rev.*, 1998, **98**, 359.
5 Special issue on Computational Transition Metal Chemistry, E. R. Davidson, *Chem. Rev.*, 2000, **100**, 351.
6 C. Fonseca Guerra, J. G. Snijders, G. Te Velde and E. J. Baerends, *Theor. Chem. Acc.*, 1998, **99**, 391and references therein.
7 A. Bridgeman and G. Cavigliasso, *Inorg. Chem.*, 2002, **41**, 1761.
8 A. Bridgeman and G. Cavigliasso, *J. Phys. Chem. A*, 2002, **106**, 6114.
9 J. M. Maestre, X. López, C. Bo, J. M. Poblet and N. Casañ-Pastor, *J. Am. Chem. Soc.*, 2001, **123**, 3749.
10 A. Bridgeman and G. Cavigliasso, submitted for publication.
11 X. López, C. Bo and J. M. Poblet, *J. Am. Chem. Soc.*, 2002, **124**, 12574.
12 B. Keita, Y. Jean, B. Levy, L. Nadjo and R. Contant, *New J. Chem.*, 2002, 1314.
13 S. A. Borshch, *Inorg. Chem.*, 1998, **37**, 3116.
14 I. A. Weinstock, J. J. Cowan, E. M. G. Barbuzzi, H. Zeng and C. L. Hill, *J. Am. Chem. Soc.*, 1999, **121**, 4608.
15 A. Tezé and G. Hervé, *J. Inorg. Nucl. Chem.*, 1977, **39**, 2151.
16 X. López, J. M. Maestre, C. Bo and J. M. Poblet, *J. Am. Chem. Soc.*, 2001, **123**, 9571.
17 X. López, C. Bo, J. M. Poblet and J. P. Sarasa, *Inorg. Chem.*, 2003, **42**, 2634.
18 A. Müller, F. Peters, M. T. Pope and D. Gatteschi, *Chem. Rev.*, 1998, **98**, 239.
19 V. W. Day and W. G. Klemperer, *Science*, 1985, **228**, 533.
20 W. A. Neiwert, J. J. Cowan, K. I. Hardcastle, C. L. Hill and I. A. Weinstock, *Inorg. Chem.*, 2002, **41**, 6950.
21 T. M. Anderson and C. L. Hill, *Inorg. Chem.*, 2002, **41**, 4252.
22 C. Daul, *Int. J. Quantum Chem.*, 1994, **52**, 867.
23 J. M. Maestre, X. López, C. Bo, C. Daul and J. M. Poblet, *Inorg. Chem.*, 2002, **41**, 1883.
24 H. Duclusaud and S. A. Borshch, *Inorg. Chem.*, 1999, **38**, 3491.
25 S. A. Borshch, H. Duclusaud and J. M. Millet, *Appl. Cat. A: General*, 2000, **200**, 103.
26 H. Duclusaud and S. A. Borshch, *J. Am. Chem.Soc.*, 2001, **123**, 2825.
27 N. Casañ-Pastor and L. C. W. Baker, *J. Am. Chem. Soc.*, 1992, **114**, 10384and references therein.
28 J. J. Borrás-Almenar, J. M. Clemente-Juan, E. Coronado and B. S. Tsukerblat, *Chem. Phys.*, 1995, **195**, 1.
29 N. Suaud, A. Gaita-Ariño, J. M. Clemente-Juan, J. Sánchez-Marín and E. Coronado, *J. Am. Chem. Soc.*, 2002, **124**, 15134.
30 E. Cadot, M. Fournier, A. Tézé and G. Hervé, *Inorg. Chem.*, 1996, **35**, 282.
31 Q. Chen and C. L. Hill, *Inorg. Chem.*, 1996, **35**, 2403.
32 J. M. Maestre, J. M. Poblet, C. Bo, N. Casañ-Pastor and P. Gómez-Romero, *Inorg. Chem.*, 1998, **37**, 3444.
33 Y. Xu, H.-G. Zhu, H. Cai and X.-Z. You, *Chem. Commun.*, 1999, 787.
34 M.-M. Rohmer, M. Bénard, E. Cadot and F. Sécheresse, in *Polyoxometalate Chemistry*, M.T. Pope and A. Müller (eds.), Kluwer Academic Publishers, The Netherlands, 2001, 117–133.
35 B. Bardin, S. V. Bordawekar, M. Neurock and R. J. Davis, *J. Phys. Chem. A*, 1998, **102**, 10817.
36 J. Y. Kempf, M.-M. Rohmer, J. M. Poblet, C. Bo and M. Bénard, *J. Am. Chem. Soc.*, 1992, **114**, 1136.
37 S. Ganapathy, M. Fournier, J. F. Paul, L. Delevoye, M. Guelton and J. P. Amoureux, *J. Am. Chem. Soc.*, 2002, **124**, 7821.
38 M.-M. Rohmer and M. Bénard, *J. Am. Chem. Soc.*, 1994, **116**, 6959.
39 M.-M. Rohmer, J. Devemy, R. Wiest and M. Bénard, *J. Am. Chem. Soc.*, 1996, **118**, 13007.
40 M.-M. Rohmer, M. Bénard, J.-P. Blaudeau, J. M. Maestre and J. M. Poblet, *Coord. Chem. Rev.*, 1998, **178–180**, 1019.
41 V. W. Day, W. G. Klemperer and O. M. Yaghui, *J. Am. Chem. Soc.*, 1989, **111**, 5959.
42 A. Bridgeman, *Chem. Phys.*, 2003, **287**, 55.
43 A. Bridgeman and G. Cavigliasso, *Chem. Phys.*, 2002, **279**, 143.